ELSEVIER

Journal of Chromatography A, 848 (1999) 443–455

JOURNAL OF CHROMATOGRAPHY A

Capillary zone electrophoresis of rigid submicron-sized particles in polyacrylamide solution
Selectivity, peak spreading and resolution

Sergey P. Radko, Andreas Chrambach*

Section on Macromolecular Analysis, Laboratory of Cellular and Molecular Biophysics, National Institute of Child Health and Human Development, National Institutes of Health, Bethesda, MD 20892-1580, USA

Received 21 December 1998; received in revised form 29 March 1999; accepted 31 March 1999

Abstract

Submicron-sized rigid particles can be separated in a size-dependent fashion by electrophoresis in free solution. Yet it has remained unknown whether the presence of polymers in the solution confers an advantage in size-dependent separation of submicron particles and their resolution. The present study addresses that question, using capillary zone electrophoresis of carboxylate modified polystyrene latex microspheres of 55, 140 and 215 nm radius in solutions of linear polyacrylamide in the M_r range of $0.4 \cdot 10^6$ to $1.14 \cdot 10^6$. Selectivity of particle separation increases in direct relation to the polymer concentration in the concentration range of 0 to 1% (w/v). Selectivity was found to increase with M_r of the polymer for the particle sets of 55/140 (nm/nm) and 140/215 (nm/nm) but to decrease with polymer M_r for the 55/215 (nm/nm) set. Peak spreading is a complex and, in the case of the largest particle, non-monotonic function of polymer concentration, with a minimum at concentrations around the entanglement threshold, c^*. Consequently, resolution of the 55/215 and 140/215 (nm/nm) sets also exhibits a maximum around the entanglement threshold while resolution for the 55/140 (nm/nm) set increases with a rise of polymer concentrations above c^*. Within the range of optimally resolving polymer concentrations there also occurs a maximum of resolution for all particle sets at a field strength in the range of 150 to 250 V cm^{-1}.

Keywords: Particles, submicron-sized; Buffer composition; Polyacrylamide; Polystyrene

1. Introduction

Capillary zone electrophoresis (CZE) is widely accepted as a tool for analytical separation of soluble substances ranging from small simple ions to such macroions as proteins and nucleic acids (e.g. [1]). Over the last decade, this technique was also found to be suitable for the separation and characterization of particulate materials (microparticles) such as organic and inorganic colloids and biological vesicles of different origin, with characteristic diameters of tens of nanometers to a few micrometers (reviewed in [2]). For colloidal particles of a similar chemical composition but differing in size, such as polystyrene latex submicron-sized spheres or silica sols, the separation was generally demonstrated to be size-dependent, with larger particles demonstrating higher electrophoretic mobilities [3–9].

*Corresponding author. Tel.: +1-301-496-4878; fax: +1-301-402-0263.

E-mail address: acc@cu.nih.gov (A. Chrambach)

0021-9673/99/$ – see front matter
PII: S0021-9673(99)00456-2

As known, the electrophoretic mobility of a charged spherical particle moving in the electric field through a medium of uniform viscosity and dielectric permittivity is a complex function of particle radius (R), thickness of the electric double layer surrounding the particle (κ^{-1}), and particle zeta-potential (ζ-potential) [10,11]. The ζ-potential is connected to the important concept of the shear surface – an imaginary surface lying in the proximity of the solid surface and forming a sheath enveloping the particle. All of the material inside of that sheath forms a kinetic unit, so that the particle migrates accompanied by a certain quantity of the surrounding liquid and the charged species it contains. Therefore, electrophoretic mobility is not governed directly by the surface charge of the particle but rather by a net charge located within the shear surface. The latter differs, in general, from the charge found, for instance, by titrating charged functional groups on the surface [10,11]. The ζ-potential is the electrostatic potential at the shear surface which, in turn, depends on the net charge and radius of the particle and the thickness of the electric double layer. For a small potential ($\zeta<25$ mV at 25°C), it may be shown (e.g. Eq. 2.3.37 of [11]), that when $\kappa R>10$, the ζ-potential at equilibrium becomes directly proportional to the net charge density independently of particle size. In the κR range of ~10 to ~100, the electrophoretic mobility of the particle of uniform ζ-potential is expected to monotonically increase with κR by ~25% according to the Henry equation (see [10,11] for the reference). Above that range, it becomes an explicit function of the zeta-potential [10,11]. The thickness of the electric double layer depends merely on the ionic strength of electrolyte solution, I, decreasing as $I^{-1/2}$. At $I\cong 0.01$, which is commonly used for electrolyte solutions in CZE, $\kappa^{-1}\cong 3$ nm [11]. Thus, for a particle of 30 nm radius or above, electrophoretic mobility might be expected to modestly increase with particle size. Yet, such increase can be greatly enhanced due to the so-called 'relaxation effect' if the ζ-potential of the particle is not small. The theoretical study on the relaxation effect was independently carried out by Overbeek and Booth and further developed by Wiersema (reviewed in [10]). They have shown that, if the particle possesses a high value of ζ-potential, the deformation of the ionic atmosphere surrounding the particle due to the particle migration in the electric field greatly contributes to the migration rate, giving rise to a strong increase in electrophoretic mobility with particle size in the range of $5<\kappa R<500$ [10] corresponding to a particle size range of 15 nm$<R<$ 1500 nm at $I\cong 0.01$.

Recently, subjecting polystyrene latex spheres in the size range of 7 to 1100 nm radius to capillary zone electrophoresis in buffered solutions of entangled linear polyacrylamide, it has been demonstrated that the size-dependent retardation of the particle by the polymer becomes electric field- and particle size range-dependent once the particle size exceeds 20 nm in radius [12]. The neutral polymers are known not to change the dielectric properties of the medium even at moderate (several %, w/v) polymer concentrations [13], on the one hand, and, on the other hand, they are not able to electrostatically interact with charged functional groups present on the particle surface. Thus, irrespectively of the physical mechanisms underlying the size-dependent electrophoretic migration of polystyrene latexes in free solutions and involving, in a complex way, their (net) surface charge or, more rigorously, ζ-potential (see above), the retardation of these particles by neutral polymers appears not to be directly surface charge-dependent but determined mostly by their size. In the size range of ~20 to ~200 nm radius, the retardation was found to progressively decrease with increasing particle size at elevated field strength [12,14,15]. Consequently, larger particles which migrate faster in free buffer are retarded less in polymer-containing buffer, allowing one to employ polymer solutions as 'sieving media' to enhance the separation of submicron-sized particles by CZE in this particular particle size range. However, it has remained unknown whether the resolution of the particles can also be improved by the addition of polymers since peak spreading increases in the presence of polymers [14,16]. Although an improvement in resolution for two polystyrene latex spheres of 93 and 205 nm diameter was demonstrated in semidilute solutions of linear polyacrylamide of $7\cdot 10^6$ molecular mass at 270 V cm^{-1} [16], the relations between selectivity, peak spreading, and resolution, on the one hand, and polymer concentration including the polymer concentration regime, polymer molecular mass, electric field

strength, length of injection zone and particle radius and concentration, on the other hand, have not previously been investigated systematically.

The present study defines the effects on the selectivity, peak spreading and resolution of linear polyacrylamide, with molecular masses ranging from $4 \cdot 10^5$ to $1.14 \cdot 10^6$, in the electrophoretic buffer in application to three negatively charged polystyrene particles (110 to 430 nm diameter) subjected to CZE at various electric field strengths, particle concentrations, and lengths of injection zone.

2. Experimental

2.1. Materials

2.1.1. Buffer

The electrophoretic buffer was a solution of 22 m*M* Tris, 22 m*M* boric acid, 0.5 m*M* Na_2EDTA (designated TB buffer), prepared by 40-fold dilution of 10×TBE buffer (0.89 *M* Tris, 0.89 *M* boric acid, 0.02 *M* Na_2EDTA, pH 8.3, BioWhittaker, Walkersville MD, USA, catalogue No. 16-012BN).

2.1.2. Particles

Particles were fluorescent (fluorescein labeled) carboxylate modified polystyrene (PS) latex spheres of 110±5, 280±7 and 430±12 nm diameter (Interfacial Dynamics, Portland, OR, USA, catalogue No. 2-FY-100,1; 2-FY-300,1; 2-FY-400,1; designated as PS-55, -140, and -215, respectively). Particles were supplied as 2% solid latex suspensions in distilled water. The suspensions were appropriately diluted to obtain samples of 0.002, 0.006, 0.02% solids in TB buffer for particles of each size. These sample concentrations correspond to particle volume fractions of $1.9 \cdot 10^{-5}$, $5.7 \cdot 10^{-5}$, $1.9 \cdot 10^{-4}$, respectively (based on a polystyrene latex density of 1.05 g ml^{-1}).

2.1.3. Polymers

Polymers were linear polyacrylamide (PA) of different molecular mass. Solid PA of nominal molecular mass (M_r) of $0.4 \cdot 10^6$, $0.6 \cdot 10^6$, $1 \cdot 10^6$, and $1.14 \cdot 10^6$ with polydispersity [weight-average molecular mass (M_w)/number-average molecular mass (M_n)] of 2.6, 2.5, 2.5, and 2.5, respectively, was obtained from Polysciences (Warrington PA, USA, catalogue Nos. 19 790, 18 259, and 18 260, lot Nos. 403 471 and 412 244; designated as PA-0.4, -0.6, -1, and -1.14, respectively). Their 1.5% (w/v) aqueous stock solutions were prepared by solubilization in deionized water with gentle shaking overnight. PA of M_r 700 000–1 000 000 and unknown polydispersity (Polysciences, catalogue No. 19 901; designated as PA-0.8) was supplied as a 10% aqueous solution. Aqueous PA solutions were appropriately mixed with the buffer concentrate to obtain the required PA concentrations within the range of 0.1%– 1.0% in TB buffer.

2.2. Capillary zone electrophoresis

Electropherograms were obtained by means of the P/ACE 2100 capillary electrophoresis system (Beckman Instruments, Fullerton CA, USA) equipped with a laser-induced fluorescence detector with excitation wavelength of 488 nm and detection wavelength of 520 nm. Experiments were performed in fused-silica capillaries of 27 or 47 cm total length, 150 μm I.D. and 360 μm O.D., externally coated with polyamide (Polymicro Technologies, Phoenix AZ, USA, catalogue No. TSP150375). The detection window was formed at 20 (27 cm total length) or 40 (47 cm total length) cm from the injection (cathodic) end of the capillary (effective capillary length), using a glowing wire to remove the external coating. Thereafter, the capillaries were internally coated with 3% uncrosslinked polyacrylamide to suppress the electroosmotic flow [17]. Capillaries were thermostated at 25°C and tested with regard to electroosmosis prior and subsequent to CZE by determining the mobility of picric acid (J.T. Baker, Phillipsburg NJ, USA, catalogue No. 0276-01) in Tris-borate buffer ($2.8 \cdot 10^{-4}$ cm^2 s^{-1} V^{-1}). Capillaries exhibiting a picric acid mobility of less than $2.7 \cdot 10^{-4}$ cm^2 s^{-1} V^{-1} were discarded.

CZE was conducted as described elsewhere [18], using PA solutions in TB buffer. The value of electric current did not exceed 38 μA even at the highest field strength used, 531 V cm^{-1}. Sample injection by pressure (3.5 kPa) was carried out taking into account the dependence of injection time on viscosity of the polymer solution as follows. Polymer solution containing a dye (SPADNS, Aldrich,

catalogue No. 11 475-8) was pressure (3.5 kPa) injected into the capillary filled with the same solution without dye. The time required by the dye to reach the detector in polymer solution (t_p) and buffer (t_o) was measured. The ratio of t_p/t_o was used to calculate both the injection time in presence of polymer providing a constant injection volume, independent of polymer concentration, and the length of the injection plug in presence of polymer at various injection times. The length of injection plug in free buffer was calculated as described elsewhere [19]. The length of injection plug was maintained at about 1.5% of the effective capillary length ($\cong 6$ mm) in all experiments unless stated otherwise.

2.3. Viscometry

Rheological measurements were carried out by means of a rotational viscometer equipped with a digital display (Model DV-I+, Brookfield Engineering Labs., Stoughton, MA, USA), using the Brookfield UL cylindrical adapter providing shear rates of 0.6 to 122 s^{-1}. The viscometer tube assembly was immersed in a thermostated bath at 25°C.

The measurements were performed as follows: 18 ml of the buffer or the PA-0.8 solution at each PA concentration used were placed into the cylindrical cell of the viscometer and allowed to temperature equilibrate for at least 10 min prior to a viscosity reading. Viscosity was measured at four different shear rates, ranging from 6.1 to 61.2 s^{-1}.

2.4. Conductimetry

Electric conductivity of the electrophoretic buffer was measured using a CDM 2d conductivity meter (Radiometer, Copenhagen, Denmark).

2.5. Data processing

The migration times corresponding to the half-heights of the ascending and descending limbs of the detected peak, t_1, and t_2, as well as the mode of the peak, t_m, were provided by the P/ACE 2100 software (Beckman, System Gold). The conversion from the 'temporal' width of a peak, $\Delta t_{1/2}=(t_2-t_1)$, with units of time, to the 'spatial' width of the peak passing through the detector position, $\Delta X_{1/2}$, used the relation:

$$\Delta X_{1/2} = \Delta t_{1/2}\,(t_m/t_1 t_2)L \quad (1)$$

where L is the effective capillary length.

Selectivity of particle separation, $\Delta\mu/\mu_{av}$, defined as [20]:

$$\Delta\mu/\mu_{av} = |\mu^A - \mu^B|/[(\mu^A + \mu^B)/2], \quad (2)$$

was calculated using the values of particle electrophoretic mobility (μ) provided by the System Gold software.

Resolution designated as ''*Res*'' was calculated as follows:

$$Res = |t_m^A - t_m^B|/(\Delta t_{1/2}^A + \Delta t_{1/2}^B) \quad (3)$$

Here superscripts A and B correspond to any set of two polystyrene particles out of the three under study. It should be noted that use of Eq. (3) implies a Gaussian peak shape. The actual shape of peaks observed in the present study sometimes clearly deviated from the Gaussian (Fig. 10). Thus, Eq. (3) did not provide accurate values of resolution in all cases under study. Yet, it appears sufficient for indicating trends in resolution as a function of polymer concentration and molecular mass or electric field strength when these are the subjects of interest. The experimental data from measurements of individual particle sizes were used to calculate selectivity (Eq. (2)) and resolution (Eq. (3)) for purposes of analysis, though the separations of mixtures of particle sizes were also performed (Fig. 1).

The intrinsic viscosity of the PA-0.8 solution was obtained by a linear extrapolation of plots, comprising values of either reduced $[(\eta_{solution}-\eta_{solvent})/\eta_{solvent}c]$ or inherent $[\ln(\eta_{solution}/\eta_{solvent})/c]$ viscosities at low PA concentrations, to infinite dilution. Here $\eta_{solution}$ and $\eta_{solvent}$ are absolute viscosities (cP) of the PA solutions and the buffer, respectively, provided by viscometry, and c is the polymer concentration (g ml^{-1}).

3. Results and discussion

3.1. Organization of polymers in solution

Polymer solutions are commonly used in CZE in

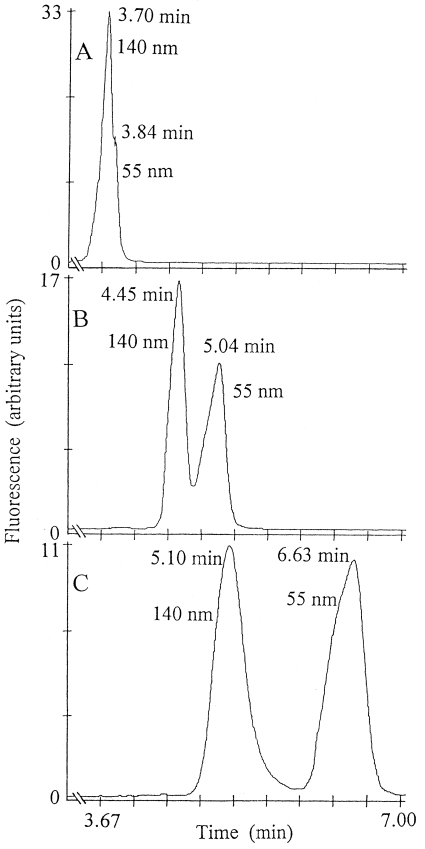

Fig. 1. Representative electropherograms. Polystyrene latex spheres of 55 and 140 nm radius, sample concentration 0.02% solid latex. CZE: 150 μm I.D. capillary of 20 cm effective capillary length, 270 V cm^{-1}, 25°C, initial zone length of ≅10 mm (≅5% of the effective capillary length). This initial zone length corresponds to 1 s injection time, the minimum tolerated by the P/ACE 2100 apparatus. (A) TB buffer alone; (B) 0.3% PA-0.8 solution in TB buffer; (C) 0.7% PA-0.8 solution in TB buffer.

two concentration regimes: dilute and semidilute (a detailed discussion of, as well as a list of relevant references on, the organization of polymers in solution and their application to electrophoretic separation may be found, e.g. in [21–23]). Briefly, when a flexible linear polymer is solubilized, its chain is known to be random-coiled. In the so-called dilute concentration regime, these polymer coils are separated in space and interact incidentally. When the polymer concentration increases, at some point (the so-called 'entanglement threshold', c^*) the polymer coils start to overlap and penetrate each other, forming a continuous spatial network due to steric interactions between polymer chains (semidilute regime). Once formed, the network is characterized by an average size of mesh which decreases with polymer concentration and is independent of polymer molecular mass.

A polymer network in solution, and therefore a transition from the dilute to the semidilute regime, can be generated either by increasing the concentration of polymers of a defined M_r, or by increasing the M_r of the polymers at a defined concentration since the entanglement threshold concentration is a reciprocal function of the zero-shear intrinsic viscosity of a polymer solution, $[\eta]$:

$$c^* = A/[\eta] \quad (4)$$

Prefactor A is equated by different authors to 1 or 1.5 (see [24] and [21], respectively, and references therein). Using the Mark–Houwink–Sakurada (MHS) equation, $[\eta]=KM_r^a$, where $a=0.8$ and $K=4.9\cdot10^{-3}$ (g^{-1}ml) for aqueous PA solutions at 25°C [25], Eq. 4 may be rewritten as follows:

$$c^* = A/KM_r^a \quad (5)$$

The viscosity values of PA-0.8 solutions were found to be independent of shear rates within the range of 6 to 61 s^{-1} at all PA concentrations used (data not shown). Therefore, the intrinsic viscosity derived by using those values would be that at zero shear rate and may be applied to calculate the entanglement threshold. The linear extrapolation to zero PA concentration of both the reduced and inherent viscosities yielded values of $[\eta]$ of 299±16 and 313±6 (g^{-1}ml), respectively. The mean value, 306 g^{-1} ml, gives values of c^* equal to ~0.3% and ~0.5% for $A=1$ and 1.5, respectively (Eq. (4)). The other approach to estimate c^* is to determine the concentration at which the double-logarithmic plot of specific viscosity, $[(\eta_{solution}/\eta_{solvent})-1]$, versus polymer concentration departs from linearity (slope=1) [26]. The departure is supposed to correspond to the progressive transition of the polymer solution into the entangled state. Since the value of $c^*\cong0.3\%$ was found to be close to such departure (data not shown), that value was taken as the crossover from dilute to semidilute concentration regimes in PA-0.8 solutions.

For PA of well-defined molecular mass, the en-

tanglement threshold can be calculated according to Eq. (5). Assuming $A=1$, for PA of the lowest M_r used, $0.4\cdot10^6$, Eq. (5) yields $c^*\cong0.7\%$. Thus, at a fixed polymer concentration of 1%, all PA solutions were entangled but approached the entanglement threshold with decreasing PA molecular mass.

3.2. Selectivity, peak width, and resolution of microparticles as a function of polyacrylamide concentration and molecular mass

An analytical separation of two components is characterized by the resolution, Res, defined in the spatial domains as follows [20]:

$$Res = \Delta X/2\,(\sigma_1 + \sigma_2) \quad (6)$$

Here ΔX is the distance between the centers of gravity of the two zones corresponding to the separands and σ_1 and σ_2 are the respective variances (assuming a Gaussian shape of the zones). Eq. (6) may be considered as a fundamental definition of resolution since, as was pointed by Giddings (p. 99 of [20]), 'the spatial disengagement in the column remains the (hidden) basis of a separation' even if zones emerge one by one at the time scale as it is in most forms of chromatography or in CZE. However, the definition of resolution in the time domain as $Res=\Delta t/(2\sigma_{t1}+2\sigma_{t2})$ is also accepted in elution chromatography (e.g. [27–29]) and CZE (e.g., [30,31]) and may be applied for practical calculations in the form of Eq. (3), with peak width at half-height ($\Delta t_{1/2}$) instead of dispersion ($2\sigma_t$). Eq. 6 was transformed by Giddings [20] into the form that allows for operating with appropriate working parameters to optimize the resolution:

$$Res = (\Delta\nu/\nu_{av})\,(N/16)^{1/2} \quad (7)$$

where $\Delta\nu$ and ν_{av} are a difference in zone velocities and their arithmetic average, respectively, N is the mean plate number (separation efficiency). For electrophoresis, Eq. (7) can be rewritten as follows [20]:

$$Res = (\Delta\mu/\mu_{av})\,(N/16)^{1/2} \quad (8)$$

Thus, the resolution is directly proportional to the selectivity (see Eq. (2)) and the square root of separation efficiency. The main drawback of Eq. (7) in application to practical calculations of resolution from the experimental data is the uncertainty in calculating the mean plate number if the peak widths sufficiently differ and (or) the peaks do not overlap [32]. Consequently, though polymer effects on the microparticles separation were analyzed in terms of selectivity ($\Delta\mu/\mu_{av}$) and peak width ($N^{1/2}=L/\sigma\sim1/\Delta X_{1/2}$ for a given effective capillary length, L), the resolution was calculated using Eq. (3) rather than Eq. (8).

Selectivity of particle separation for polystyrene particle sets of 55/140, 55/215 and 140/215 (nm/nm) was found to increase monotonically with increasing PA-0.8 concentration within the limits of experimental scatter, albeit at different rates for different sets. Representative plots of selectivity as a function of PA concentration (at an electric field strength, E, of 270 V cm^{-1}) are shown in Fig. 2. An increase in selectivity with PA concentration was observed for all particle concentrations studied, with relatively slight variations in values of selectivity with particle (sample) concentration. The plots for each particle set were reproducible within the limits presented in Fig. 2 as variations in selectivity with sample concentration. The variations are thought to result from a decrease in particle retardation by polymers with increasing sample concentration that occurs at different rates for microparticles of different size [15]. Though the effect of sample concentration on particle mobility was found to be much weaker than that of particle size [15], the variation in sample concentration can affect the selectivity in different directions for different particle sets since the selectivity depends on both the absolute values of mobilities (μ_{av}) and their differences ($\Delta\mu$). At a PA concentration of 1%, selectivity of particle separation increases with increasing PA molecular mass for the 55/140 and 140/215 (nm/nm) sets of particles while decreasing in the same range of polymer M_r for the 55/215 set. This appears to reflect the finding reported earlier that, at a given PA concentration, the electrophoretic mobility of polystyrene microspheres decreases with increasing PA molecular mass at different rates for particles of different size [15]. Representative plots for selectivity as a function of the M_r of the polymer at a PS concentration of 0.02% are shown in Fig. 3.

Peak width for all particles under study exhibits an overall increase with increasing PA-0.8 concentra-

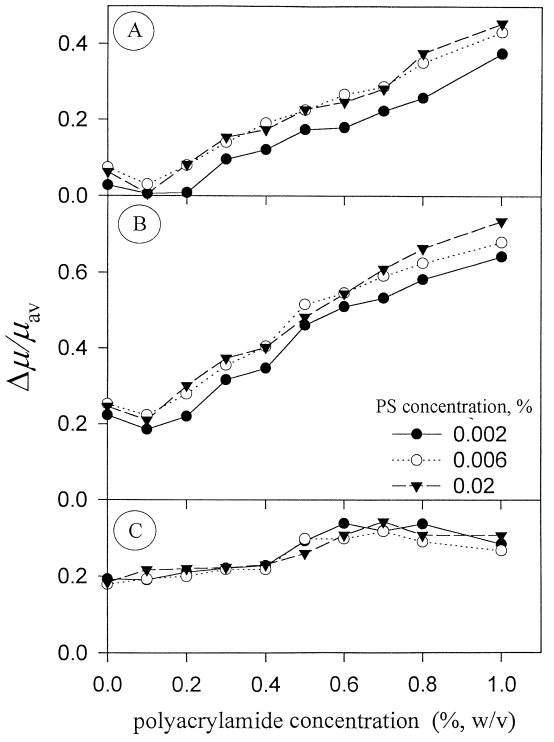

Fig. 2. Representative plots of selectivity of particle separation for carboxylate modified polystyrene latex microspheres (sets of particles of 55 and 140, 55 and 215, 140 and 215 nm radius) at various particle concentrations (0.002, 0.006, and 0.02%, w/v, of solid latex) as a function of PA-0.8 concentration. CZE: 150 μm I.D. capillary of 40 cm effective length, 270 V cm^{-1}, 25°C, initial zone length of ≅6 mm (≅1.6% of the effective capillary length). Lines are drawn to guide the eye.

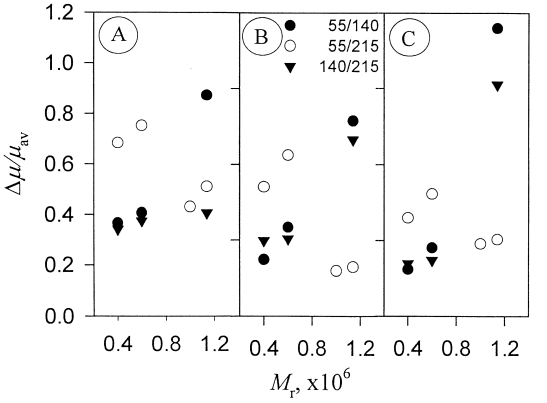

Fig. 3. Representative plots of selectivity of separation of polystyrene microparticles as a function of polyacrylamide molecular mass. Polymer concentration of 1% (w/v); particle concentration of 0.02% (w/v) of polystyrene solid latex. Electric field strengths: (A) 43 V cm^{-1}; (B) 270 V cm^{-1}; (C) 530 V cm^{-1}. Other conditions as in Fig. 2.

tion. However, both rates and patterns of this increase differ depending on particle size and concentration (Fig. 4). While $\Delta X_{1/2}$ of PS-55 shows a moderate monotonic increase independently of particle concentration throughout the PA concentration range used (Fig. 4A), peak width of PS-140 increases monotonically but at different rates depending on particle concentration: the rate is independent of PS concentration at PA concentrations below c^* and sharply rises with decreasing particle concentration at PA concentrations above it (Fig. 4B). By contrast, for PS-215, $\Delta X_{1/2}$ exhibits a steady increase, independently of particle concentration, with increasing PA concentration above c^* while exhibiting a complicated pattern below that concentration, with a peak width monotonically decreasing with PA con-

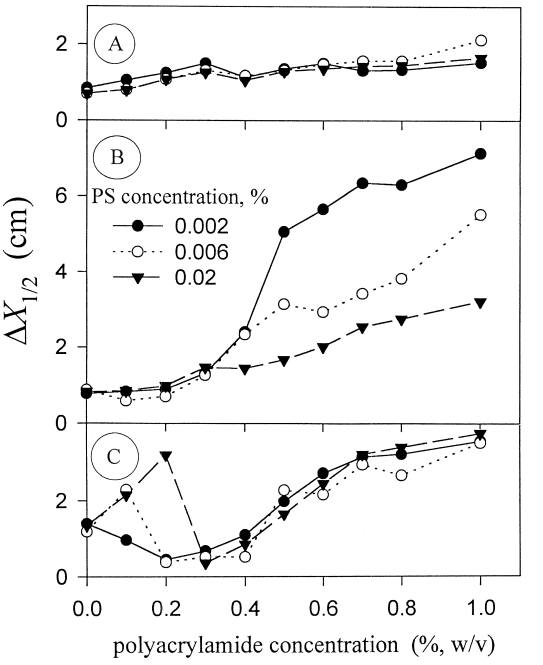

Fig. 4. Peak width for polystyrene microparticles of various size versus PA-0.8 concentration at various particle concentrations (PS concentration, %, w/v). Particle radius: (A) 55 nm; (B) 140 nm; (C) 215 nm. Other conditions as in Fig. 2. Lines are drawn to guide the eye.

centration at a PS concentration of 0.002% and undergoing a biphasic transition at higher PS concentrations (Fig. 4C). It should be noted that though the observed biphasic transition is qualitatively reproducible, the absolute values of $\Delta X_{1/2}$ at a PS concentration of 0.02% in the PA concentration range of 0.1 to 0.2% are widely variable. This variability is thought to reflect a complex dependence of the final width and shape of peak on both the initial zone length and PS concentration (Fig. 10, 3A–C) and the fact that small variations in the length of initial zone are hard to control experimentally. The effects of the initial zone length on peak width and shape will be discussed in the Section 3.4. At a concentration of c^* (about 0.3%), peak width of PS-215 is shown to be at a minimum at all PS concentrations used (Fig. 4C). At a PA concentration of 1%, peak width increases with PA molecular mass for all particles (Fig. 4). The peak width is not affected by electric field strength for PA of higher molecular mass but exhibits some dependence on E for PA of smaller polymer M_r, at least for the largest particles under study (Fig. 5).

The dependencies of resolution on polymer concentration (Fig. 6) reflect the complex relations between peak width and PA concentration (Fig. 4). In the cases of two sets of particle resolution, 55/215 and 140/215, resolution is maximal at PA concentrations around c^*. Only resolution of the 55/140 set remains steady or slightly improves beyond c^* (Fig. 6A). At a fixed PA concentration (1%), resolution of all particle sets studied shows an improvement, within experimental scatter, with decreasing M_r of PA or, in other words, with the approach toward the entanglement threshold concentration (Fig. 7). Thus, when one is faced with selecting an optimally resolving polymer concentration for an unknown in the size range under consideration, it appears reasonable to select a concentration close to c^*. In all cases studied, the optimum of resolution near c^* exceeds the resolution in the absence of polymer by a factor of 1.5 to 2. It should also be noted that an improvement in resolution, brought about by polymers, can be expected to be much greater if particles possess significantly different

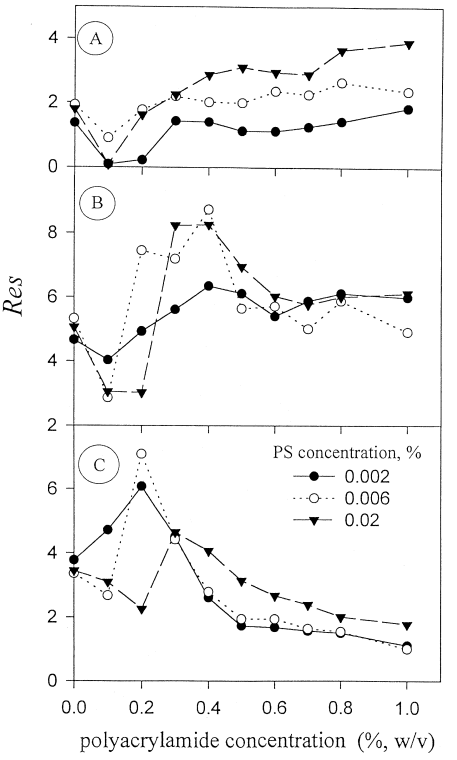

Fig. 6. Resolution of polystyrene latex microparticles at various particle concentrations (PS concentration, %, w/v) as a function of PA-0.8 concentration. Sets of particles (radius over radius, nm/nm): (A) 55/140; (B) 55/215; (C) 140/215. Other conditions as in Fig. 2. Lines are drawn to guide the eye.

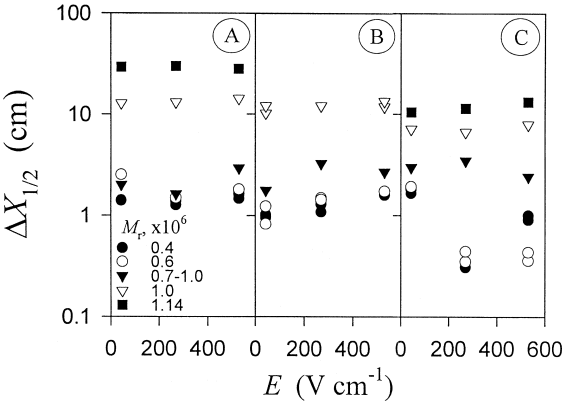

Fig. 5. Peak width for polystyrene microparticles of various size versus applied electric field strength. Polyacrylamide concentration of 1% (w/v), particle concentration of 0.02% (w/v) solid latex. Polymer molecular mass as shown in (A). Other conditions as in Fig. 2.

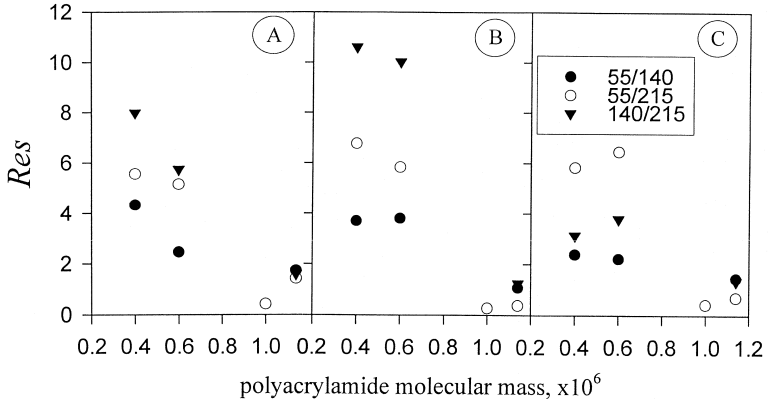

Fig. 7. Resolution of polystyrene microparticles versus polyacrylamide molecular mass. Polymer concentration of 1% (w/v); particle concentration of 0.02% (w/v) solid latex. Sets of resolved particles as shown in (A). Electric field strengths: (A) 43 V cm^{-1}; (B) 270 V cm^{-1}; (C) 530 V cm^{-1}. Other conditions as in Fig. 2.

sizes but similar electrophoretic mobilities due to, for example, particular values of their zeta-potentials. Another example for such a situation may be found in the electropherograms presented in Fig. 1. In that case, particles of the 55/140 set were not resolved in TB buffer alone (Fig. 1A), presumably due to both a shorter capillary length (20 cm) and a wider initial zone ($\cong$10 mm). Yet, complete resolution was achieved under these conditions if polymers were admixed to the electrophoretic buffer (Fig. 1B and C).

As was demonstrated earlier, the retardation of microparticles subjected to electrophoresis in polymer solutions depends on both field strength and particle size [12]. Recently, a hypothetical mechanism to account for the observed decrease in retardation with an increase in both particle size and electric field strength in the particle size range close to that under consideration has been proposed [15,16]. The mechanism implies (i) a local shear-like deformation of the polymer network, if such is formed, upon particle passage, as well as (ii) a polymer depletion in the vicinity of the particle surface, which is progressive with increasing particle radius. How such a mechanism may be related to observed dependencies for peak spreading is not clear. Yet, it appears that the peak spreading, at least for the PS-140 and -215, does not result purely from a heterogeneity in size. Such heterogeneity could hardly account for the increase in the rate of peak spreading with decreasing PS concentration for PS-140, as well as for the complex patterns of peak spreading for the particle of 215 nm radius (Fig. 6B and C).

3.3. Effect of electric field strength on peak width and resolution

At a PA-0.8 concentration of 0.4%, in the optimally resolving polymer concentration range close to c^*, peak width was found to be minimal in the range of field strengths of 150 to 200 V cm^{-1} (Fig. 8B) for the entire particle size range under study. In free buffer (Fig. 8A), the same minimum of peak width can be observed around 300 V cm^{-1} for all but the 140 nm radius particle whose peak width declines steadily with increasing field strength. Corresponding to the minima of peak width (Fig. 8B), one finds maxima of resolution at 150–250 V cm^{-1} for the 55/140, 55/215 and 140/215 sets in 0.4% PA-0.8 solution (Fig. 9).

Can the dependence of peak width on field strength be accounted for by Joule heating, at least at the highest values of electric field applied? Joule heating is known to give rise to peak spreading in electrophoresis even in the absence of convection, by generating a temperature gradient inside the capillary. The mathematical treatment of the contribution of the temperature gradient, $\sigma^2_{\Delta T}$, to peak spreading provides the following expression [33]:

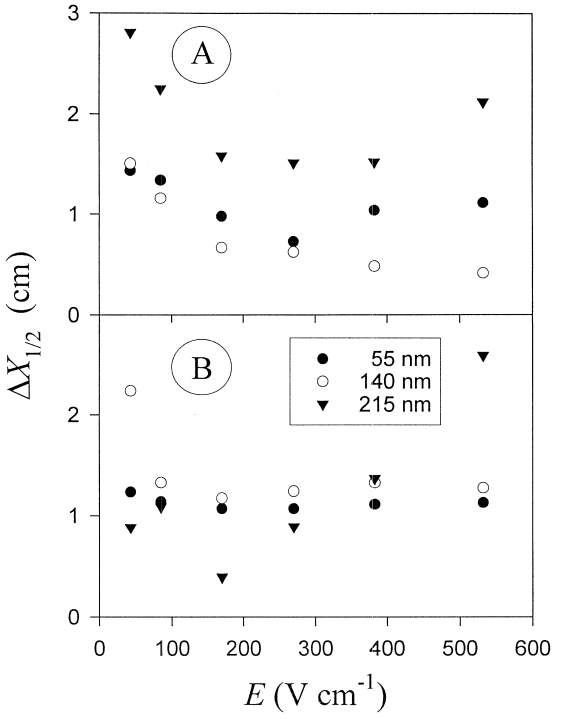

Fig. 8. Peak width for polystyrene microparticles of various sizes as a function of applied electric field strength. Particle concentration: 0.02% (w/v) of solid latex. (A) TB buffer alone; (B) 0.4% PA-0.8 solution in TB buffer. Other conditions as in Fig. 2.

$$\sigma^2_{\Delta T} = r^6 E^5 k^2 \theta^2_T \mu L / 1536 D k^2_T$$

Here r, k, θ_T, μ, L, D, and k_T are the capillary inner radius, buffer conductivity, temperature coefficient of electrophoretic mobility, electrophoretic mobility of analyte, capillary effective length, diffusion coefficient of the analyte, and buffer thermoconductivity, respectively. It is usually assumed that contributions of all of the various sources of peak spreading in term of variance, σ^2, are independent of one another and consequently additive. Thus, albeit small values of the diffusion coefficient of large particles abolish the contribution to peak spreading due to ordinary diffusion ($\sigma^2_d = 2DL/\mu E$), such 'smallness' of D can greatly increase the peak spreading due to the temperature gradient. The diffusion coefficient of polystyrene particles may be estimated according to Stokes–Einstein law: $D = k_B T / 6\pi\eta R$, where k_B, T, η, and R are the Boltzmann constant, the absolute temperature (298 K), absolute viscosity of medium

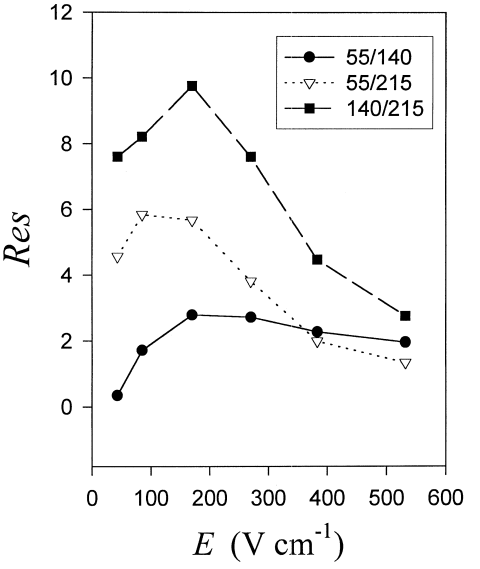

Fig. 9. Resolution of polystyrene microparticles versus applied electric field strength. PA-0.8 concentration: 0.4% (w/v); particle concentration: 0.02% (w/v) of solid latex. Other conditions as in Fig. 2. Lines are drawn to guide the eye.

(0.9 cP for the buffer and 2.9 cP for 0.4% PA-0.8 solution), and particle radius, respectively. The conductivity of TB buffer at 25°C was measured as 0.0094 Ω^{-1} m^{-1}. Values of θ_T and k_T are known from the literature [34]: $\theta_T = 0.02$ K^{-1} and $k_T = 0.006$ W cm^{-1} K^{-1} if taken as that of water. The values of $\sigma^2_{\Delta T}$, calculated according to Eq. 6 for $E = 530$ V cm^{-1}, and corresponding total variances estimated as $(\Delta X_{1/2})^2/5.54$ are listed in Table 1. Both the estimation of a total variance by $(\Delta X_{1/2})^2/5.54$ and comparison with calculated $\sigma^2_{\Delta T}$ values assume a Gaussian peak shape that, rigorously speaking, is not

Table 1
Calculated variance due to the temperature gradient inside the capillary, $\sigma^2_{\Delta T}$, and estimated total variance, $(\Delta X_{1/2})^2/5.54$, of peaks of polystyrene latex microparticles in CZE at field strength of 530 V cm^{-1}

Particle radius (nm)	PA-0.8 concentration			
	0%		0.4%	
	$\sigma^2_{\Delta T}$ (cm^2)	$(\Delta X_{1/2})^2/5.54$ (cm^2)	$\sigma^2_{\Delta T}$ (cm^2)	$(\Delta X_{1/2})^2/5.54$ (cm^2)
55	0.01	0.22	0.05	0.22
140	0.03	0.04	0.12	0.31
215	0.05	0.87	0.19	1.32

always found (e.g. Fig. 10). However, the comparison of $(\Delta X_{1/2})^2/5.54$ with $\sigma^2_{\Delta T}$ may be accepted as a rough estimate of an effect of the temperature gradient on peak spreading. It is seen (Table 1) that peak spreading at 530 V cm^{-1} due to the temperature gradient may account for a large part of the final peak width of PS-140 but not for that of particles of the other sizes. Since $\sigma^2_{\Delta T} \sim E^5$, the contribution of the temperature gradient to the observed peak width may be shown to be negligible for particles of all sizes under study at lower values of the field strength (Fig. 8).

Can the dependence of peak spreading on field strength be accounted for by 'electrophoretic heterogeneity'? Here the 'electrophoretic heterogeneity' of polystyrene latex implies its naturally non-uniform electrophoretic mobility due to a heterogeneity in particle size and net charge density, complicated by a distortion of the ionic atmosphere of the particle by the electric field. Heterogeneity of electrophoretic mobility has been suggested by Petersen and Ballou [6] as a dominant source of zone spreading in free solution CZE of microparticles. The suggestion was based on the independence of separation efficiency on electric field strength in the range of 100 to 600 V cm^{-1} observed by those authors for carboxylated PS particles of 35 and 50 nm radius [6]. The spatial peak width (and, therefore, the separation efficiency) for particles of 55 nm radius shows a slight variation with E within the range of 150 to 550 V cm^{-1} in the present study as well (Fig. 8A). However, that of PS-140 and -215 depends on field strength more acutely. Particles of all sizes demonstrated an increase in $\Delta X_{1/2}$ at $E < 100$ V cm^{-1}.

The increase of peak width with decreasing field strength (below 100 V cm^{-1}) is unlikely to be a pure sedimentation effect due to increasing migration time. At least for PS-55, there was no sedimentation observed even during a few days of storage at rest. One may speculate that the extent of the relaxation effect, i.e. a distortion of the ionic atmosphere surrounding the particle as it electrophoretically migrates through the electrolyte solution, can affect a 'degree of electrophoretic heterogeneity' of particle populations resulting in variation of peak width with E. Aside from the electrophoretic heterogeneity, one can also not rule out that an interaction between particles and capillary walls may contribute to peak

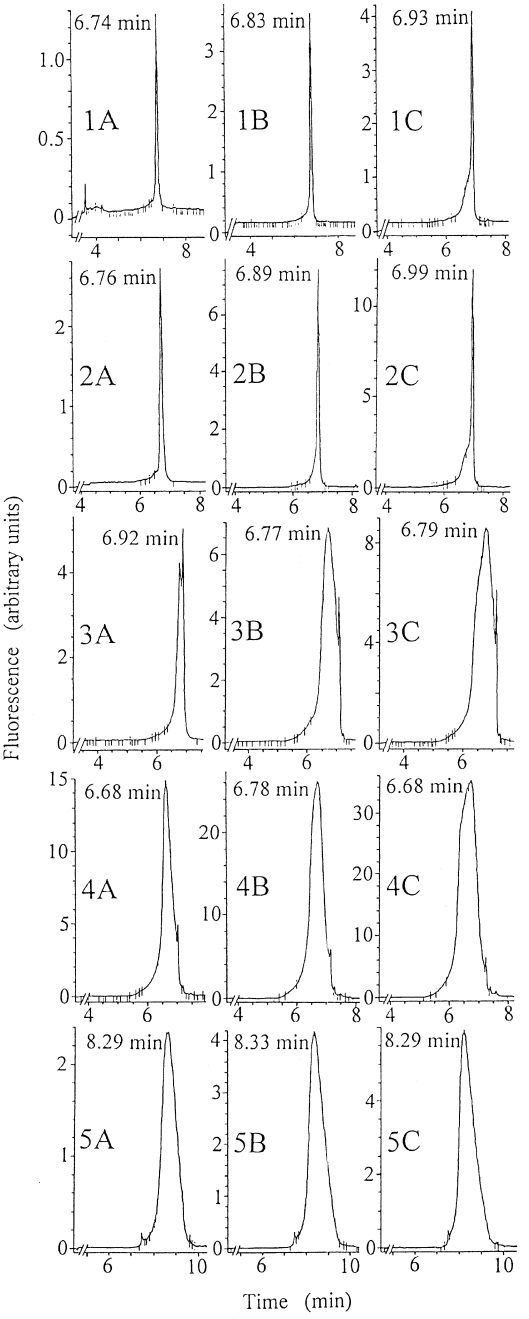

Fig. 10. Electropherograms of 215 nm microparticles at various lengths of the initial zone, particle and PA-0.8 concentrations. Initial zone length: Column A: ≅4 mm; Column B: ≅7 mm; Column C: ≅11 mm. Particle concentration: rows 1 to 5: 0.002, 0.006, 0.02, 0.06 and 0.02% (w/v) of solid latex, respectively. Polymer concentration: rows 1 to 4: 0.2% (w/v), and row 5-0.8% (w/v) PA-0.8 solution, respectively. Other conditions as in Fig. 2.

spreading in a size- and field strength-dependent manner. Note that such an interaction has been only ruled out when spatial zone width is independent of voltage [6]. Since in the present study such voltage dependence has been demonstrated (Fig. 8A), interaction with the walls remains a possibility.

The peak spreading in free buffer differs for particles of different size (Fig. 8A). Irrespective of mechanisms responsible for this field strength-dependent peak spreading of microparticles of a given size in free buffer, the dependencies of peak spreading on E are definitely changed by the presence of the polymer chains in the electrophoretic buffer (Fig. 8A versus B and Fig. 8A versus Fig. 5). Thus, the interaction of microparticles with polymers, when subjected to CZE in a polymer solution, not only gives rise to the size- and field strength-dependent retardation [12,15,16] but also contributes to size- and field strength-dependent peak spreading. Beyond a statement of this fact, a discussion of mechanisms responsible for the particle's peak spreading in polymer solutions appears to be even more speculative at the present time than that regarding the peak spreading in free buffers in view of the limited volume of available experimental data.

3.4. Effects of initial zone length on peak width and shape

The experimental relations described by Figs. 2–9 have been derived from CZE data which used a common initial zone length held around 1.5% ($\cong$6 mm) of the effective capillary length (L). Variation of initial zone length (ΔL) within the range of 1 to 3% of L did not change the peak width to any appreciable extent for particles of 55 nm radius throughout the PA concentration range used (data not shown). For PS-140 the peak width remained unchanged below c^* while for PS-215 it remained unchanged above c^* (data not shown). For PS-140, at PA concentrations above c^*, peak width increased with decreasing length of the initial zone. For example, at a PS concentration of 0.02% and a PA concentration of 1%, $\Delta X_{1/2}$ increased by a factor of $\cong$1.5 when $\Delta L/L$ decreased from 3 to 1% (data not shown). One may conclude that length of initial zone, if held within a few percents of effective capillary length, does not contribute much to a final peak width of microparticles of 55 to 140 nm radius, subjected to electrophoresis in PA solutions. For PS-140, the total load rather than the length of the initial zone or particle concentration appears to affect peak spreading at PA concentrations above c^*.

For particles of 215 nm radius, at PA concentrations below c^* where peak width depends on PS concentration at a fixed initial zone length (Fig. 4C), the relationships between initial zone length, particle concentration and both width and shape of peaks are more complex. Thus, at a PA concentration of 0.2%, both width and shape of peaks do not change much upon increase in PS concentration from 0.002 to 0.006% at a fixed initial zone length (Fig. 10, rows 1 to 2 for each of columns A, B, and C) but peak shape definitely deforms with increasing $\Delta L/L$ from 1 to 3% at a fixed PS concentration (Fig. 10, columns A to C, rows 1 and 2). In both cases (increase in initial zone length or in PS concentration), the total load (the number of particles) is increased by a factor of 3. Yet, when the PS concentration range increases from 0.002%–0.006% to 0.02%–0.06% (Fig. 10, 3A–4C), the peaks are broadening significantly. Moreover, their trailing limb is sharpening, giving rise to a narrow additional subpeak. In some cases, the pattern may look like a double peak (Fig. 10, 3A). Upon increase of PA concentration to 1%, peaks becomes broad, near-Gaussian, and independent of ΔL in the range studied (Fig. 10, 5A–C).

4. Conclusions

Dependencies of peak width and peak shape of submicron-sized particles on polymer and particle concentration, polymer and particle size, strength of applied electric field and initial zone length appears to be much more complex than those for mobilities, making, at least at the present time, any theoretical discussion highly speculative. However, it cannot be ruled out that the mechanisms of peak spreading of submicron-sized particles electrophoresed in polymer solutions are the same as those governing their retardation.

The main practical conclusions which can be derived from this study are as follows. The polymer solutions can enhance or bring about the resolution

when particles in the size range of 50 to 140 nm radius are separated by CZE. The resolution increases with increasing polymer concentration. In this particle size range, the increase in sample concentration can result in increasing resolution, contrary to the general expectation. When the particle size range is extended to 220 nm radius, the admixture of polymers to the electrophoretic buffer at a concentration near the entanglement threshold, c^*, provides an improvement in resolution at the optimal field strengths of 150 to 250 V cm^{-1}. It should be noted that for any given polymer, c^* can readily be estimated from its nominal M_r since $c^* \cong 1/KM_r^a$, where K and a are constants for the given specific polymer and solvent.

References

[1] J.P. Landers (Ed.), Handbook of Capillary Electrophoresis, CRC Press, Boca Raton, FL, 1994.
[2] S.P. Radko, A. Chrambach, J. Chromatogr. B 722 (1999) 1.
[3] B.B. VanOrman, G.L. McIntire, J. Microcol. Sep. 1 (1989) 289.
[4] H.K. Jones, N.E. Ballou, Anal. Chem. 62 (1990) 2484.
[5] R.M. McCormick, J. Liq. Chromatogr. 14 (1991) 939.
[6] S.L. Petersen, N.E. Ballou, Anal. Chem. 64 (1992) 1676.
[7] B. VanOrman-Huff, G.L. McIntire, J. Microcol. Sep. 6 (1995) 591.
[8] A.B. Hlatshwayo, C.A. Silebi, Polym. Mater. Sci. Eng. 75 (1996) 55.
[9] U. Schnabel, C.-H. Fischer, E. Kenndler, J. Microcol. Sep. 9 (1997) 529.
[10] J.Th.G. Overbeek, P.H. Wiersema, in: M. Bier (Ed.), Electrophoresis: Theory, Methods, and Applications, Vol. II, Academic Press, New York, 1967, p. 1, Ch. 1.
[11] R.J. Hunter, Zeta Potential in Colloid Science: Principles and Applications, Academic Press, London, 1981.
[12] S.P. Radko, A. Chrambach, Electrophoresis 17 (1996) 1094.
[13] D.E. Brooks, G.V.F. Seaman, J. Colloid Interface Sci. 43 (1973) 670.
[14] S.P. Radko, A. Chrambach, Electrophoresis 19 (1998) 1620.
[15] S.P. Radko, A. Chrambach, Macromolecules 32 (1999) 2617.
[16] S.P. Radko, A. Chrambach, Electrophoresis 19 (1998) 2423.
[17] S. Hjerten, J. Chromatogr. 347 (1985) 191.
[18] S.P. Radko, M.M. Garner, G. Caiafa, A. Chrambach, Anal. Biochem. 223 (1994) 981.
[19] S.P. Radko, G.H. Weiss, A. Chrambach, J. Chromatogr. A 781 (1997) 277.
[20] J.C. Giddings, Unified Separation Science, Wiley, New York, 1991.
[21] J.-L. Viovy, C. Heller, in: P.G. Righetti (Ed.), Capillary Electrophoresis in Analytical Biotechnology, CRC Press, Boca Raton, FL, 1996, p. 478.
[22] M.A. Quesada, Curr. Opin. Biotechnol. 8 (1997) 82.
[23] J.-L. Viovy, T. Duke, Electrophoresis 14 (1993) 322.
[24] C.N. Onyenemezu, D. Gold, M. Roman, W.G. Miller, Macromolecules 26 (1993) 3833.
[25] P. Molyneux, in: Water-Soluble Synthetic Polymers: Properties and Behavior, Vol. 1, CRC Press, Boca Raton, FL, 1983, p. 84.
[26] P.D. Grossman, D.S. Soane, J. Chromatogr. 559 (1991) 257.
[27] J.M. Miller, Chromatography: Concepts and Contrasts, Wiley, New York, 1988.
[28] J.C. Giddings, in: E. Heftmann (Ed.), Chromatography: A Laboratory Handbook of Chromatographic and Electrophoretic Methods, 3, Van Nostrand Reinhold, New York, 1975, pp. 27–45.
[29] B.L. Karger, J. Gas Chromatogr. 5 (1967) 161.
[30] E. Kenndler, W. Friedl, J. Chromatogr. 608 (1992) 161.
[31] A. Luckey, L.M. Smith, Anal. Chem. 65 (1993) 2841.
[32] A.S. Said, Sep. Sci. Technol. 13 (1978) 647.
[33] R. Virtanen, Acta Polytech. Scand. 123 (1974) 7.
[34] P.D. Grossman, in: P.D. Grossman, J.C. Colburn (Eds.), Capillary Electrophoresis: Theory and Practice, Academic Press, San Diego, CA, 1992, p. 32.